

1      **Distinct functional responses of producers and their  
2      consumers to climate shape trophic asymmetry in  
3      mutualistic networks**

4      **Gabriel Munoz<sup>1</sup>, Paul Savary<sup>1</sup>, W. Daniel Kissling<sup>2</sup>, JP Lessard<sup>1</sup>**

5      <sup>1</sup>Concordia University,  
6      <sup>2</sup>University of Amsterdam,

7      **Abstract**

8      Functional traits are often used to infer the ecological processes that determine the  
 9      composition of species assemblages. Whereas most trait-based approaches to infer  
 10     community assembly processes focus on a single trophic level, traits also mediate  
 11     interactions between trophic levels. Owing to the matching of traits facilitating in-  
 12     teractions between producer and consumer assemblages, the functional trait diversity  
 13     of different trophic levels is expected to covary in space. However, the differential  
 14     response of consumers and producers to environmental gradients can cause a decou-  
 15     pling of functional diversity between trophic levels, which we coin functional trophic  
 16     asymmetry. Here, we develop a metric to quantify functional trophic asymmetry  
 17     (FTA) and use it to infer the processes underpinning multitrophic community as-  
 18     sembly and explore the role of these processes in shaping the topology of ecological  
 19     networks.

20     We used digitally available data on the functional traits, pairwise mutualistic interac-  
 21     tions, and geographic distributions of consumers (mammalian frugivores) and their  
 22     producers (palms) to quantify FTA for species assemblages occurring in the Neotrop-  
 23     ics. To cover major data gaps between species-level trait and interaction data at  
 24     finer spatial grain, we trained machine learning models to downscale the continental  
 25     meta-network to grid cell-level networks. For each grid-cell, we also estimated FTA  
 26     for all combinations of interaction guilds. These guilds were defined as distinct sub-  
 27     sets of producer and consumer assemblages playing similar roles within mutualistic  
 28     networks and sharing partners in the other trophic level. We then used generalized  
 29     additive models to relate geographic variation in FTA to variation in climatic vari-  
 30     ables and assessed whether the strength of these relationship varied among pairwise  
 31     interaction guilds. Finally, we then examined the relationship between FTA and  
 32     network specialization across 1,072 grid cells in the Neotropics.

33     Our approach to model mutualistic network assembly identified 7 consumers x pro-  
 34     ducer interaction guilds. Assemblage-wide FTA was negatively related to annual  
 35     mean temperatures across the neotropics. When considering individual interaction  
 36     guilds, precipitation seasonality was positively related to FTA. This relationship  
 37     between FTA and precipitation seasonality was stronger for consumer and pro-  
 38     ducer guild combinations with high predicted interaction strength. Finally, network  
 39     specialization was positively related to FTA, regardless of the interaction guild com-  
 40     bination.

41     Mutualistic networks in warm regions with seasonal rainfall, where the environment  
 42     imposes a disproportionately strong selective pressure on palms relative to mammal  
 43     frugivores, exhibit higher levels of functional trophic asymmetry. This relationship is  
 44     particularly strong when considering guilds predicted to strongly interact in nature.  
 45     Assemblages exhibiting high FTA also tend to have high levels of network special-  
 46     ization, suggesting that differences in the strength of environmental selection among  
 47     trophic levels favor the persistence of specialist species in these mutualistic interac-  
 48     tion networks. We therefore conclude that future increases in temperature and the  
 49     magnitude of precipitation seasonality caused by global climate change could lead to  
 50     more specialized mutualistic networks which are more prone to collapse when facing  
 51     further threats and local extinctions.

52      **0.1 Introduction**

53      Ecologists often examine patterns of functional trait diversity to investigate com-  
 54      munity assembly processes (Ackerly, 2003; Kraft et al., 2015). To date, however,  
 55      trait-based approaches in ecology often focus on a single trophic level, whereas ap-  
 56      proaches that consider multiple trophic levels remain rare (Lavorel, 2013; Seibold  
 57      et al., 2018). An approach that considers processes operating within and between  
 58      trophic levels is necessary to better understand the assembly of multitrophic com-

59 munities (Allesina et al., 2008; Marjakangas et al., 2022; Saravia et al., 2022). More-  
 60 over, considering trophic interactions while studying community assembly could shed  
 61 new light on processes underpinning ecological networks (Allesina et al., 2008). Clas-  
 62 sical approaches to study community assembly rely on the concept of environmental  
 63 filtering, sorting or selection, where density independent conditions constrain the  
 64 functional richness of species assemblages (HilleRisLambers et al., 2012; Kraft et al.,  
 65 2015; Laliberté & Legendre, 2010; Villéger et al., 2008). Functional richness refers  
 66 to the variability and relative frequency of different functional traits observed in a  
 67 community. It is often used to estimate the strength of selection imposed by the  
 68 environment (Kraft et al., 2008, 2015; Kraft & Ackerly, 2010). High functional richness  
 69 can indicate weak environmental selection whereas low functional richness can  
 70 indicate strong selection (Halpern & Floeter, 2008; Kraft et al., 2008; Paine et al.,  
 71 2011). In a multitrophic context, the effects of environmental selection can cascade  
 72 across trophic levels such that selection on consumer traits can shape the functional  
 73 richness of their resources, modulated by their degree of reciprocal dependency or  
 74 co-evolution (Lavorel, 2013). Moreover, the same environmental gradient could exert  
 75 selective pressures of different strength on communities at distinct trophic levels  
 76 (Marjakangas et al., 2022). Differences in the strength of selective pressure among  
 77 trophic levels could then possibly constrain the structure or topologies of trophic  
 78 networks (Blüthgen et al., 2007; Dehling et al., 2021; Schleuning et al., 2012)

79 Inferring the relative strength of environmental selection between trophic levels re-  
 80 quires using high-dimensional approaches that can deal with sparse observations for  
 81 many species (Rohr et al., 2010; Strydom et al., 2022). We introduce the concept of  
 82 functional trophic asymmetry (FTA), which allows inferring the relative influence  
 83 of environmental selection and trait matching on the composition of multitrophic  
 84 assemblages (Figure 1). FTA is the difference in the richness of interaction-relevant  
 85 traits between trophic levels in a multitrophic network. FTA can occur because  
 86 traits mediating species interactions (i.e., interaction niches) across trophic levels  
 87 can also mediate the responses of species to their abiotic environment (i.e., environ-  
 88 mental niches) (Dehling et al., 2021; McCain & King, 2014; Moretti & Legg, 2009).  
 89 As an example, plant seed size determines the outcome of animal-mediated seed dis-  
 90 persal (Donoso et al., 2017, 2020) as well as physiological limits, such as tolerances  
 91 of plant seedlings to desiccation (Hoekstra et al., 2001). High FTA could indicate  
 92 differences in the strength of environmental selection over the interaction niches of  
 93 distinct trophic levels within a multitrophic species assemblage. Alternatively, low  
 94 FTA could indicate that the strength of the environment selection shaping inter-  
 95 action niches is similar between trophic levels, e.g., equally weak or equally strong  
 96 (Marjakangas et al., 2022). When interactions between producers and consumers are  
 97 mutualistic, low FTA could also emerge under strong trait matching and therefore  
 98 indicate the influence of trait co-evolution during multitrophic community assembly  
 99 (Albrecht et al., 2018; Dehling et al., 2021). By studying spatial variation in FTA  
 100 along environmental gradients, we could possibly identify the conditions promoting  
 101 environmentally versus cross-trophic interaction- driven community assembly (Bello  
 102 et al., 2023).

103 Frameworks linking multitrophic functional diversity to network topology along  
 104 broad-scale environmental gradients are crucial to understand the effects of global  
 105 change on biodiversity and ecosystem function (Bello et al., 2023; Dehling et al.,  
 106 2021; Schleuning et al., 2012). Functional responses of consumer and producer as-  
 107 semblages to climate influence functional richness at the level of the multitrophic  
 108 community (García et al., 2018). Because some of these traits are involved in inter-  
 109 actions across trophic levels, the filtering of traits along environmental gradients  
 110 could constrain the identity, number, and frequency of species interactions and  
 111 therefore, network topology (Albrecht et al., 2018; Emer & Memmott, 2023; Mar-  
 112 jakangas et al., 2022). As an example, constraints of varying intensities along cli-

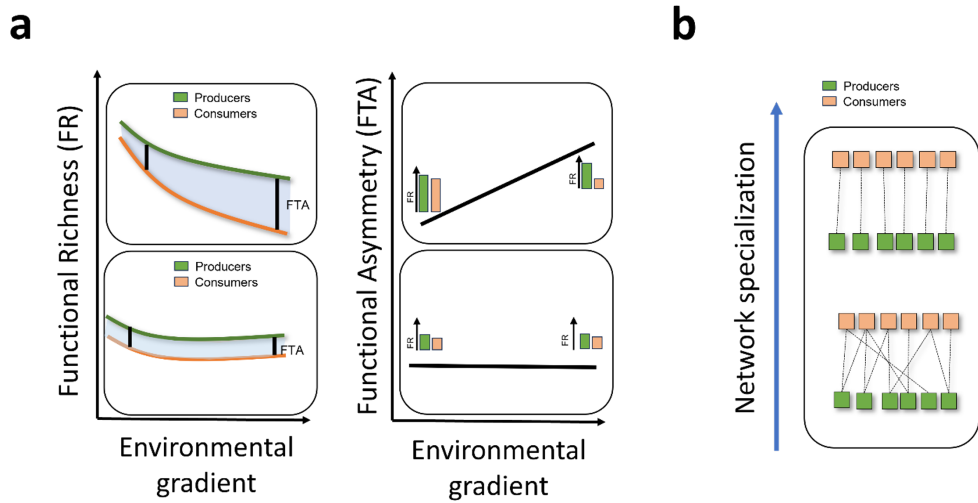


Figure 1: This conceptual model illustrates the dynamic relationship between functional diversity metrics—specifically Functional Richness (FR) and Functional Trait Asymmetry (FTA)—and environmental gradients within ecological networks. The left panel of Figure a) visualizes the variation in FR for producers (depicted in green) and consumers (depicted in orange) along an environmental gradient. As the environmental gradient intensifies (e.g., through changes in temperature, precipitation, or habitat fragmentation), FR for both producers and consumers generally decline. However, this decline can occur at different rates, leading to two scenarios: (1) Differential Decline in FR: If consumer FR declines more sharply than producer FR, a substantial increase in Functional Trait Asymmetry (FTA) occurs. (2) Parallel Decline in FR: Alternatively, if both producer and consumer FRs decline at a similar rate, FTA remains relatively constant along the gradient. This scenario indicates a balanced impact of environmental changes across trophic levels, preserving the relative functional relationship between producers and consumers. Figure b) shifts focus to the implications of changing FTA on network specialization—a measure of how distinct generalized interactions are between producers and consumers within ecological networks.

113 matic gradients, which limit the relative availability of interaction partners across  
 114 trophic levels, could influence emergent patterns in network structure such as the  
 115 specialization of multispecies interactions (Blüthgen et al., 2006, 2007; Marjakangas  
 116 et al., 2022). While high levels of network specialization represent networks pre-  
 117 dominantly made of “one-to-one” interactions, low levels of network specialization  
 118 represent networks with species showing predominantly “one-to-many” interactions  
 119 (Blüthgen et al., 2006; Blüthgen & Klein, 2011) ([Figure 1B](#)). One highly expected  
 120 outcome is that when functional trophic asymmetry is high, networks will have low  
 121 specialization. For example, take a plant community exhibiting a low richness of  
 122 flower displays and which is associated with a bee community (pollinators) exhibit-  
 123 ing a wide variety of proboscis lengths. These plants are unlikely to form “one-to-  
 124 one” interactions with only a subset of bee species that have matching proboscis  
 125 length. Otherwise, non-matching pollinators would have no food resources and be ex-  
 126 tirpated. By partitioning deviations from expected FTA and network specialization  
 127 relationships with null models, one can separate the relative influences of processes  
 128 operating between trophic levels (e.g. trait matching) and those within trophic lev-  
 129 els (e.g. environmental selection) in network assembly (Marjakangas et al., 2022).  
 130 However, the relationship between network specialization and functional trophic  
 131 asymmetry has not been fully explored.

132 Preserving mutualistic interactions between palms and their mammalian frugivores  
 133 is important to sustain biodiversity and ecosystem function in the tropics (Bogoni  
 134 et al., 2020; Marques Draxler & Kissling, 2022). Mammalian frugivores facilitate  
 135 the dispersal of palm fruits, which helps to prevent local extinctions amid distur-  
 136 bance and to maintain biodiversity in these ecological networks (Acevedo-Quintero  
 137 et al., 2020; Dehling et al., 2022; Messeder et al., 2021). To effectively preserve these  
 138 interactions, it is crucial to understand how co-occurring palm (producer) and mam-  
 139 malian frugivore (consumer) communities respond to environmental gradients. By  
 140 examining co-variation in their functional richness across broad geographic scales  
 141 and linking those patterns to spatial and/or temporal variation in climate, we can  
 142 identify key abiotic factors that influence the assembly of their mutualistic relation-  
 143 ships. Here, we ask (1) *which climatic variable(s) best explains geographic variation*  
 144 *in the functional richness of palms and mammal frugivores*, (2) *whether differences*  
 145 *in these relationships lead to functional trophic asymmetry* (hereafter FTA), and (3)  
 146 *which climatic variable best explains geographic variation in FTA across the Neotrop-*  
 147 *ics*. We also ask (4) *whether the strength of interactions between palm-frugivore*  
 148 *interaction guilds relates to the strength of the relationship between FTA and cli-*  
 149 *mate*. Finally, we ask (5) *whether geographic variation in FTA relates to network*  
 150 *specialization*.

## 151 0.2 Methods

### 152 0.2.1 Study system

153 We focused on multitrophic communities of Neotropical palms and their mutualis-  
 154 tic, seed dispersing, mammalian frugivores [Figure 2](#). Palms (Plantae:Areceae) are  
 155 a keystone plant family in tropical regions that provides fruit resources to a wide  
 156 variety of vertebrate frugivores, including birds and mammals (Muñoz et al., 2019).  
 157 Frugivore mammals (Animalia:Mammalia) are among the most important palm-  
 158 seed dispersers, particularly over long distances. Most frugivore mammals feeding  
 159 on palms are seed eaters and pulp eaters, dispersing palm seeds mostly via ectozoo-  
 160 chorous dispersal (Messerder et al., 2021). Importantly, frugivory-related traits have  
 161 notably underlain palm diversification and played a key role in the evolution of palm  
 162 traits (Kissling et al., 2012; Onstein et al., 2014, 2017).

### 163 0.2.2 Data sources

#### 164 0.2.2.1 Geographic distribution data

We obtained binary species distribution data (present/absent) on palms from the geographic range maps of (Bjorholm et al., 2005) and on mammals from the IUCN (International Union for the Conservation of Nature) data portal. To generate local gridded multitrophic species assemblages across the Neotropics, we intersected the species-level range maps with a spatial grid where each grid cell represented every 1 by 1 degree latitude and longitude change along the extent of the entire Neotropics. We then listed all palm and mammal frugivore species co-occurring in each grid-cell as our grid-cell level multitrophic assemblage.

#### *0.2.2.2 Trait data*

We collected species-level multitrophic trait data related to the physiological tolerance of palms and frugivorous mammals to the abiotic environment and to their mutualistic interactions. For palms, we extracted data from the PalmTraits 1.0 dataset (Kissling et al., 2019). We collected data on growth form, maximum stem height, and average fruit length. For frugivorous mammals, we obtained trait data from the EltonTraits 1.0 database (Wilman et al., 2014). We selected data on body mass, diet, and daily activities. Diet data from the EltonTraits 1.0 database is coded as percentage use distribution across ten diet categories. We excluded from our analysis species without fruit in their diet. Activity was coded as a dummy variable with three categories (Diurnal, Crepuscular, Nocturnal). Finally, body mass was coded as a numerical variable in kg. We excluded bats from the analysis as almost no Neotropical bat species is feeding on palm fruits (Messeder et al., 2021). From this dataset, we selected only those species whose range in gridded multitrophic communities within a regular  $1 \times 1^\circ$  latitude grid co-occur with at least 5 other palm and mammal frugivore species in the same grid. In total, we worked with a subset from this dataset of 494 palm species and 488 mammal frugivore species with linked trait and geographic data. Pairwise interaction data

We used data on seed dispersal interactions between palms and mammals for the Neotropics, originating from recollections of seed dispersal records found in the published literature and interaction records are recorded at the species level (Muñoz et al., 2019). Each pairwise species interaction record reflects where an article mentions the fruit or the seed of a palm being dispersed, carried or defecated by a frugivorous mammal. Interaction records collected in this database were previously vetted to reflect effective seed dispersal interactions, while avoiding those that reflect mere seed consumption (vetting criteria found in: Muñoz et al. (2019) ). In total, we gathered a total of 581 interaction records between 69 palms and 111 frugivore mammals.

#### *0.2.2.3 Environmental data*

We used bioclimatic variables from WorldClim (Fick & Hijmans, 2017) to represent large-scale spatial and temporal variation of climate in the Neotropics. Specifically, we used mean annual temperature (BIO01), total annual precipitation (BIO12), temperature seasonality (BIO04) and precipitation seasonality (BIO15). Using a moving window, we compute simple averages for every set of bioclimatic records at each grid cell, thereby re-scaling the spatial resolution of bioclimatic variables to 1 by 1 degree grid resolution from their original resolution ( $1 \times 1 \text{ km}^2$ ) to match the spatial resolution of our grid cell species-level data Figure 2

#### *0.2.3 Statistical analysis*

Building a probabilistic continental metaweb from aggregated binary interaction records Here, we fitted latent variable network structural models that vary in their assumptions to estimate interaction probabilities from observed binary data on species interactions. (Figure 3) Specifically, we tested: the stochastic block model (SBM), the connectance model, the trait-matching model, and the matching-centrality model (Terry & Lewis, 2020). The SBM assumes that ecological networks are modular, with species of consumers interacting more within their preferred groups of producers (i.e., interaction guilds). This model outputs three incidence

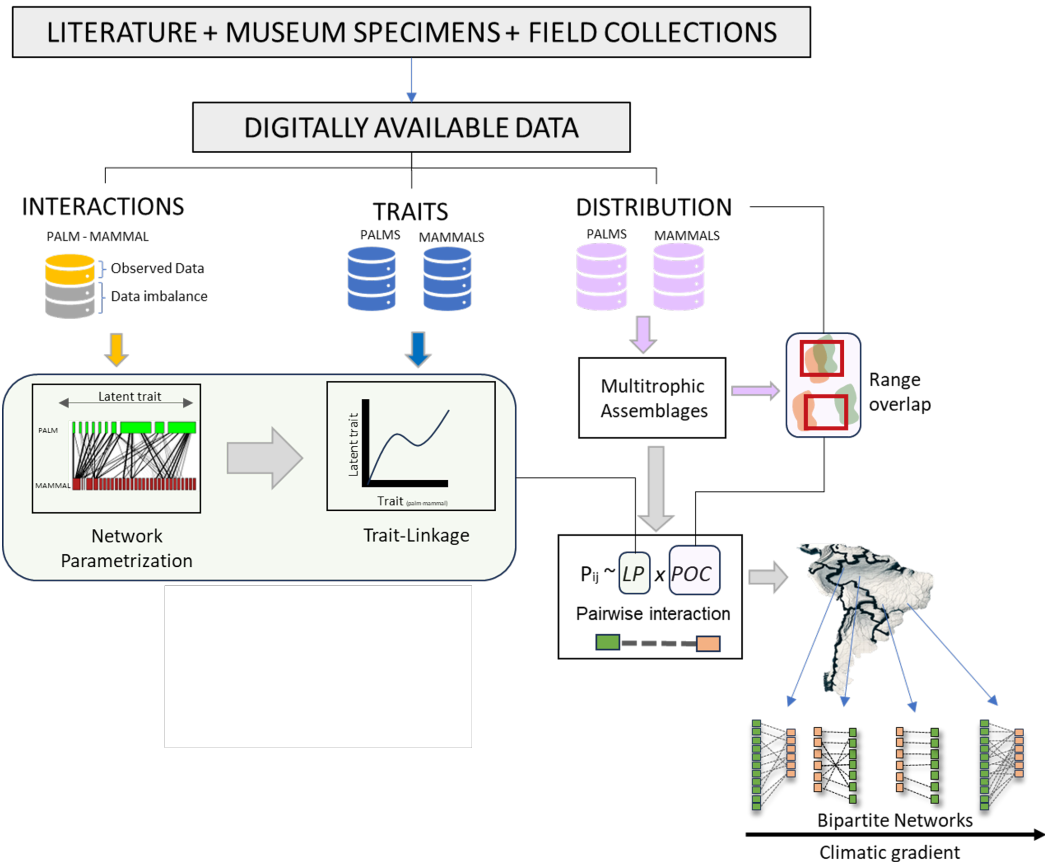


Figure 2: Workflow illustrating the integration of ecological and trait data from digital sources to model species interactions and predict ecological networks across geographic regions. The figure illustrates a workflow for integrating ecological interaction data derived from literature, museum specimens, and field collections into digitally available datasets. These datasets are used to build ecological network models and link species interactions to their biological traits. The approach involves parameterizing networks based on latent traits and identifying trait-linkages, which are subsequently utilized to predict ecological interactions and networks across different geographic locations (e.g. The Neotropics)

matrices, reflecting predicted interactions: (i) one with guilds of palm species based on their modular interactions with mammals, (ii) a similar one for mammals, and (iii) one representing the interaction probabilities (Theta) among the guilds of each group (i.e., palm guilds-mammal-guild). The connectance model posits that interactions of specialist species are subsets of those of generalist species, optimizing connectivity scores to recreate observed network patterns. The trait-matching model assumes non-random species interactions determined by trait differences, optimizing parameters along latent-trait axes. The matching-centrality model combines connectivity scores and latent-trait axes (Terry and Lewis 2020). We fitted these models to our available interaction data and selected the model that best predicted the observed continental pattern of seed dispersal interactions. Using Youden's J as a metric that balanced model sensitivity and specificity (Poisot, 2023), we found that the SBM was the best supported model Figure 3 and therefore focused on it in the rest of the manuscript. Additional details about the model assumptions are explained in Supplementary Text S1.

#### 0.2.3.1 Identifying interaction guilds

Since the hyperparameters of the Stochastic Block Model (SBM) provided the best fit for capturing the observed interactions, palm-frugivore interaction networks are highly modular and certain groups of producers are more likely to interact with certain groups of consumers than others, and vice versa. In this context, we define an interaction guild as a distinct group of palm and mammal species within the continental metaweb that exhibits similar interaction patterns. Within each guild, both producer and resource species perform comparable functional roles in the network. Within and between each guild combination of consumers and producers, species pairs exhibit the same interaction strength, where interaction strength is defined as the magnitude or intensity of the effect that one species has on another within an ecological network. Here we estimate interaction strength as the probability that a species pair would interact in nature. The SBM estimates such interaction probabilities based on the frequency of interactions observed between species assigned to given guild of consumer or producer. The SBM model uses maximum likelihood to adjust the number of guilds and the distribution of interaction probabilities within and between guilds such that they best explain the observed pattern of interactions. Using SBMs largely reduces the complexity of dealing with interaction strengths by treating them as a guild-level phenomenon instead of a species-specific one.

#### 0.2.3.2 Downscaling the continental metaweb to generate grid-cell level networks

The digital availability of primary biodiversity data on palms and their mammalian frugivores was imbalanced, with a high availability of distribution ranges and species traits, but a limited number of interaction records. Therefore, to downscale our initial metaweb to include interactions between every potentially co-occurring palm and mammal frugivore in every grid cell across the Neotropics, we used a twofold approach Figure 2.

First, we employed multinomial logistic regression models to predict the species level SBM model results (i.e., interaction guild affiliation) from species-level trait data. We justify the choice of multinomial logistic regression models as these can handle the prediction of non-binary outcomes, such as the labeling of interaction guilds per species. We fitted separate multinomial models for palms and mammal frugivores using a label backpropagation algorithm and a neural network engine, with 75% of the data allocated for training and the 25% remaining for testing. We use neural networks because they are useful when dealing with multicollinearity, as they can learn complex and non-linear relationships and interactions among multiple predictor variables. This allowed us to separate the relative importance of distinct matching traits on SBM group affiliations. We extracted variable importance scores based on the combinations of the absolute values of the best fit model weights (Gevrey et al., 2003)

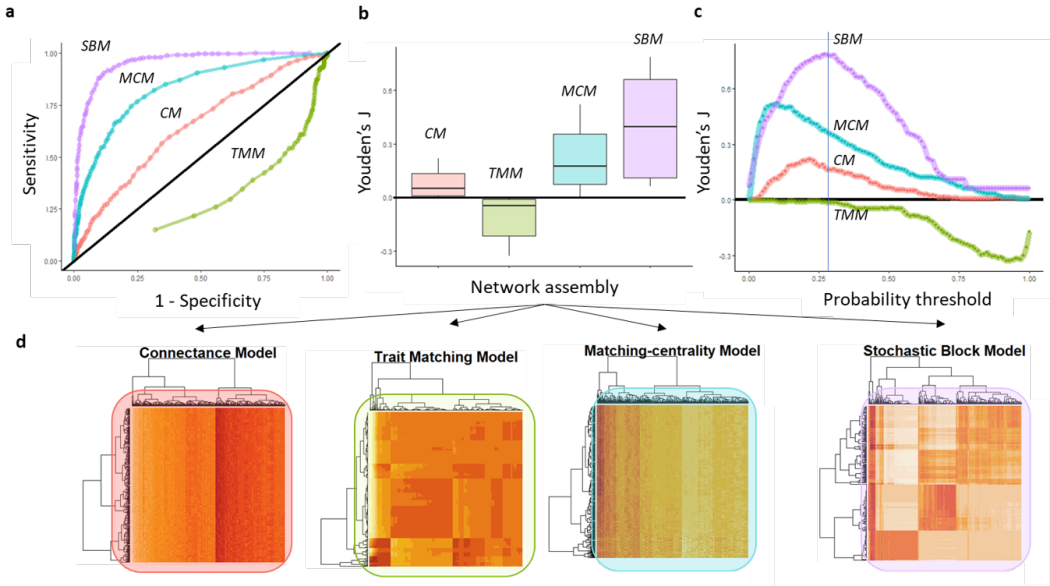


Figure 3: Model evaluation plots of distinct structural models fitted to predict the structure of the observed palm-mammal frugivore interactions in the Neotropics. In this figure we illustrate a comparison of ecological network assembly models using ROC curves (a), Youden's J index (b,c), and clustering heatmaps (d) to illustrate differences in predicting species interactions. Specifically, the figure compares four ecological network assembly models—Centrality Model (CM), Trait Matching Model (TMM), Matching Centrality Model (MCM), and Stochastic Block Model (SBM)—in their ability to accurately predict a observed binary pattern of species interactions. For our study, this observed pattern reflected the incidence of seed dispersal interactions between palms and their mammalian frugivores. The ROC curves (a) indicate model performance in terms of model sensitivity (i.e. true positive rate) versus model specificity (true negative rate). Curves further above the diagonal demonstrate stronger predictive ability, showing that the model performs significantly better than random guessing in identifying ecological interactions. If a ROC curve is close to or below this diagonal, the model's predictive performance is no better than random chance. The central boxplot summarizes the Youden's J index, where higher values reflect higher overall predictive accuracy. Panel (c) shows Youden's J index variation over different probability thresholds to materialize binary interactions. The heatmaps below visualize clustering patterns, highlighting structural differences in predicted interaction networks for each model.

Second, we considered local pairwise species interaction probabilities as the product of the values from the Theta matrix from the SBM model that represent the latent interaction probabilities between species pairs within and between groups multiplied by their probability of co-occurrence (POC) in a grid cell. To represent species' co-occurrence probabilities, we used the reciprocal distance between the centroids of species pair ranges within the grid-cell, divided by the sum of their range areas within the grid-cell. This implied that within each grid cell, species with closer range centroids and larger cumulative areas are more likely to co-occur and interact. This approach allowed us to recreate synthetic probabilistic plant-mammal frugivore networks for each grid-cell across the Neotropics, while accounting for the heterogeneity of species ranges within each grid.

#### *0.2.3.3 Estimating Functional Richness*

We investigated the spatial variation in the relative distribution of species counts of producers and consumers across all guilds in a grid cell, as an interaction network-level indicator of the spatial distribution of producer and consumer species' functional richness. We estimated functional richness (FR) from the results of the SBM model fit, specifically, from the matrices representing the interaction guilds. Thus, to measure functional richness for each trophic level, we calculated a grid-cell level vector representing the number of species across all interaction guilds ( $n = 7$ ). To account for the differences in the total number of palm and mammal species across grid cells, we normalized this vector to the total sum of palm or mammal species counts within each grid cell.

#### *0.2.3.4 Estimating Functional Trophic Asymmetry (FTA)*

We quantified functional trophic asymmetry (FTA) as the absolute difference between the functional richness vectors across trophic levels. Since each palm and mammal species in every grid cell had the potential to be affiliated with any of the seven interaction guilds and to interact with any species from the opposite trophic level both within and between guilds, we derived one FTA measures for each grid cell, and for each pairwise palm-mammal guild combination (Figure S2).

#### *0.2.3.5 Estimating Network Specialization (H2')*

We estimated network specialization for each grid cell using the metric H2'. H2' is a network-level index that varies between 0 and 1 (Blüthgen et al. 2007). High values indicate networks that are more specialized, meaning that species from one trophic level interact with only or few species in the opposite trophic level. Low H2' values indicate that there is a low specificity of interactions in the network, meaning that species from one trophic level interact with multiple species at the other trophic level. Because inferred networks varied in their network size (i.e., number of unique interactions between palms and mammals), we rarefied the computation of H2' to networks for each grid cell such that they would all have the same size (i.e., number of interactions). Specifically, we rarefied all networks to 100 pairwise interactions and repeated the procedure 999 times to get a distribution of rarefied H2' values (Terry & Lewis, 2020). We then selected the median of this H2' distribution as our grid cell-level measure of network specialization.

#### *0.2.3.6 Assessing the influence of climate on FTA*

To assess whether climate has an influence on FTA, we fitted a Generalized Additive Model (GAM) to examine the relationships between FTA and four continuous bioclimatic predictors. The GAM approach allows for modelling flexible non-linear relationships between the predictors and the response variable using smoothed functions (Wood, 2017). The predictor variables included in our models were Mean annual temperature (Temp), Total annual precipitation (Prec), Temperature seasonality (TS), and Precipitation seasonality (PS). Collectively, are these climatic factors known contemporary factors influencing both the regional and global diversity of

324 plants and mammals (Holt et al., 2018). We fitted separate splines for each of the  
 325 climatic predictors.

326 Assessing how interaction strength mediates the influence of climate on FTA To  
 327 assess whether the strength of interaction between producer and consumer guilds  
 328 mediate the strength of the relationship between FTA and climate, we included in-  
 329 teraction strength as an interaction term in the GAM, allowing splines between FTA  
 330 and climate to vary non-linearly depending on interaction strength.

### 331 0.2.3.7 Assessing the relationship between FTA and H2'

332 We used Generalized Additive Model (GAM) to investigate the relationship be-  
 333 tween rarefied grid cell network level specialization (H2') as a response variable and  
 334 FTA (z-scores) as the main predictor. We also added the effect of Mean annual  
 335 temperature, Total annual precipitation, Precipitation seasonality, and Tempera-  
 336 ture seasonality as covariate functions because these climate variables may influence  
 337 H2' independently of FTA, allowing us to isolate the specific impact of FTA on  
 338 H2' while controlling for the indirect effects of climate on FTA. Here, we estimated  
 339 grid-cell level functional trophic asymmetry (FTA') by summing the FTA values  
 340 across all interaction guilds, weighted by their respective interaction strengths. This  
 341 approach was selected as accounts for the uneven contributions of each guild to net-  
 342 work structure, highlighting whether changes in network specialization are primarily  
 343 driven by shifts in FTA within the more specialized interaction guilds.

## 344 0.3 Results

### 345 0.3.1 Interaction guild delineation

346 The Theta matrix derived from the SBM (Stochastic Block Model) analysis Figure 4  
 347 reflects the modular pattern assumed by this model, here identified as the best for  
 348 frugivore-mammal interactions. Therefore, these interactions are stronger within  
 349 rather than between guild pairs. Given the associations found with the theta matrix,  
 350 we can derive that the following high-level trait-trait associations: a) Tall palms with  
 351 medium-sized fruits can associate strongly with small to medium sized mammals  
 352 that consume moderate to high amounts of fruit. b) Acaulescent or small-stemmed  
 353 palms with small to large fruits correlate strongly with either small, moderately  
 354 frugivorous mammals or small mammals with relatively low frugivory. Finally, c)  
 355 medium-sized to large sized mammals with moderate to low frugivory levels interact  
 356 with species with intermediate palm traits (e.g., moderately tall erect palms with  
 357 medium-sized fruits) (Figure S1).

### 358 0.3.2 The influence of climate on functional richness

359 At the grid-cell level, when ignoring interaction guild affiliations, neither the func-  
 360 tional richness of palms or mammals relates to geographic variation in climate (Fig-  
 361 ure S3,S4, Table S1,S2). The functional richness of palms does not relate to temper-  
 362 ature ( $F = 3.00$ ,  $P < 0.05$ ), precipitation ( $F = 1.19$ ,  $P = 0.23$ ), temperature season-  
 363 ality ( $F = -0.27$ ,  $P = 0.79$ ) or precipitation seasonality ( $F = 0.68$ ,  $P = 0.50$ ). The  
 364 functional richness of mammals positively relates to mean annual temperature ( $F =$   
 365  $10.60$ ,  $P < 0.05$ ) but not to precipitation ( $F = 0.001$ ,  $P = 1.00$ ), temperature season-  
 366 ality ( $F = 0.52$ ,  $P = 0.60$ ) or precipitation seasonality ( $F = 1.67$ ,  $P = 0.10$ ). When  
 367 considering guild affiliation in our analyses, there are marked differences in the re-  
 368 lationship between functional richness and climate among trophic levels (Figures  
 369 4a,4b). The functional richness of palm positively relates to precipitation seasonality  
 370 for guilds 5 ( $F = 5.62$ ,  $P < 0.01$ ) and negatively relates to precipitation seasonality  
 371 for guild 6 ( $F = 8.37$ ,  $P = 0.01$ ) (Figure S3). In contrast, the relationship between  
 372 the functional richness of mammals and precipitation seasonality does not vary  
 373 among guilds. However, the relationship with temperature does vary among guilds.  
 374 Specifically, the functional richness of guild 3 positively relates to temperature ( $F =$   
 375  $11.21$ ,  $P < 0.01$ ) whereas that of other guilds does not relate to temperature (Figure  
 376 S4).

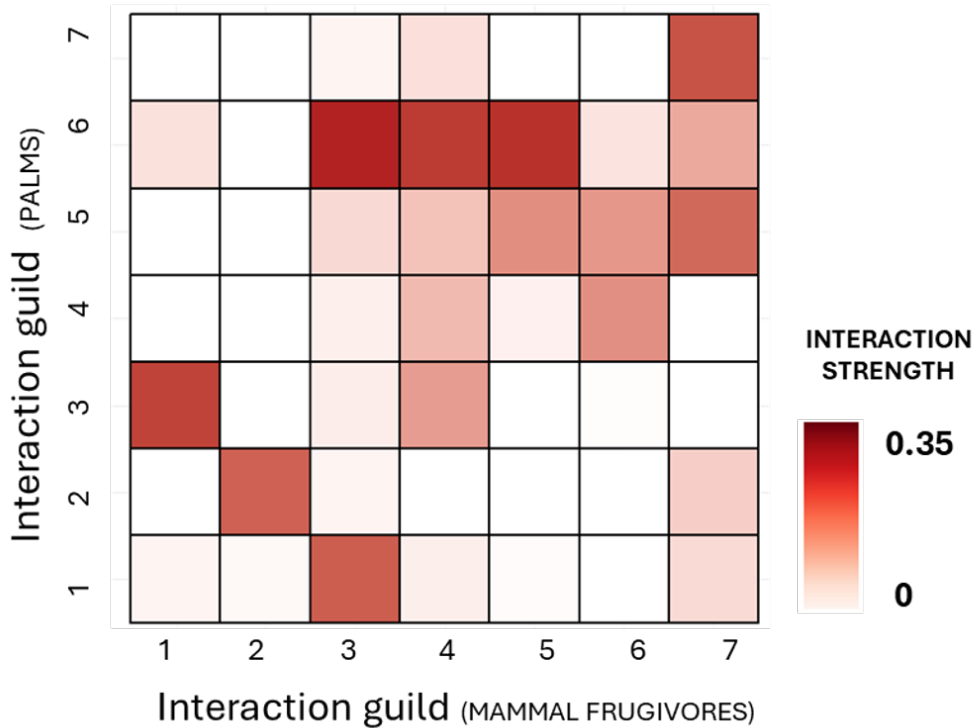


Figure 4: Heatmap depicting the probability of interaction between palm and mammal interaction guilds defined as blocks by the Stochastic Block Model (SBM). The intensity of red shading correlates with the strength of these interactions, where darker shades signify higher probabilities of interaction between species within or between interaction guilds (SBM blocks), where the probability was inferred using the Stochastic Block Model's estimated interaction parameters (theta Matrix) derived from fitting the model to observed binary (presence = 1, absence = 0) interaction data compiled from scientific literature.

**Table 1**

Source: Article Notebook

**Parametric coefficients**

	Estimate	Std. Error	t value	p-value
Intercept	0.21	0	271.5	>0.001 ***

Source: Article Notebook

**Smooth Terms**

	edf	Ref.df	F	p-value
Mean Annual Temperature	1.00	1	5.97	<b>0.01 *</b>
Mean Annual Temperature x interaction strength	0.00	27	0.00	<b>0.57</b>
Precipitation seasonality	1.00	1	0.30	<b>0.59</b>
Precipitation seasonality x interaction strength	1.67	27	0.14	<b>0.05.</b>
Temperature seasonality	1.00	1	0.19	<b>0.67</b>
Temperature seasonality x interaction strength	0.00	27	0.00	<b>0.54</b>
Total Annual Precipitation	1.00	1	0.28	<b>0.60</b>
Total Annual Precipitation x interaction strength	0.00	27	0.00	<b>0.47</b>
Interaction strength	5.00	5	746.20	>0.001 ***

Source: Article Notebook

377

**0.3.3 The influence of climate on FTA**

The distribution of functional trophic asymmetry (FTA) exhibited a bi-modal pattern, with a primary cluster centered around local maxima of FTA = 0.09 and a secondary cluster near a second local maxima of FTA = 0.49. A similar clustering pattern after standardizing FTA by the strength of interaction guilds, however, the cluster of low FTA values due to low or minimal interaction strength is more apparent (Figures 4c, 4d). The distribution of FTA varies significantly across interaction guilds (Figure S5) The maximum FTA record across all guilds was 0.93. Within individual guilds, the highest FTA values were associated with interactions between tall, erect palms bearing medium to large fruits (guild 3) and highly frugivorous mammals (guild 1) (Figure S5). Similarly, medium-sized palms with small to medium fruits (guild 5) interact with large mammals exhibiting low levels of frugivory (guild 6) also contributed significantly to high FTA standardized values In contrast, interactions involving acaulescent or short-stemmed palms with medium-sized fruits (guild 6) and small mammals with limited frugivory intake (guild 3) consistently yielded the lowest FTA standardized values (Figure S5) When ignoring interaction guilds, functional trophic asymmetry (FTA) is positively related to mean annual temperature ( $F = 5.97$ ,  $P = 0.01$ ). FTA is not related to precipitation ( $F = 0.28$ ,  $P = 0.13$ ), precipitation seasonality ( $F = 0.30$ ,  $P = 0.59$ ) or temperature seasonality ( $F = 0.19$ ,  $P = 0.67$ ) (Table 1). When considering interaction guild affiliation in our analyses, there are marked differences in how temperature (Temp) and Precipitation seasonality (PS) interact among distinct interaction guild combinations Figure 5. Specifically, an increase in the relative richness of frugivores with low levels of fruit in their diet (i.e. mammal interaction guilds 3, 6 and 7) with increasing Temperature drove changes in FTA along the temperature gradient (Figure 5a, 5c), while along increasing precipitation seasonality, FTA was driven by the reduction in the rich-

ness of short palms with low to medium fruit sizes (guild 5) and of tall palms with low fruit sizes (guild 2), coupled with an increase in the relative richness of short stemmed and acaulescent palms with medium to large fruits (guild 6) across the climatic gradient (Figure 5b,5d).

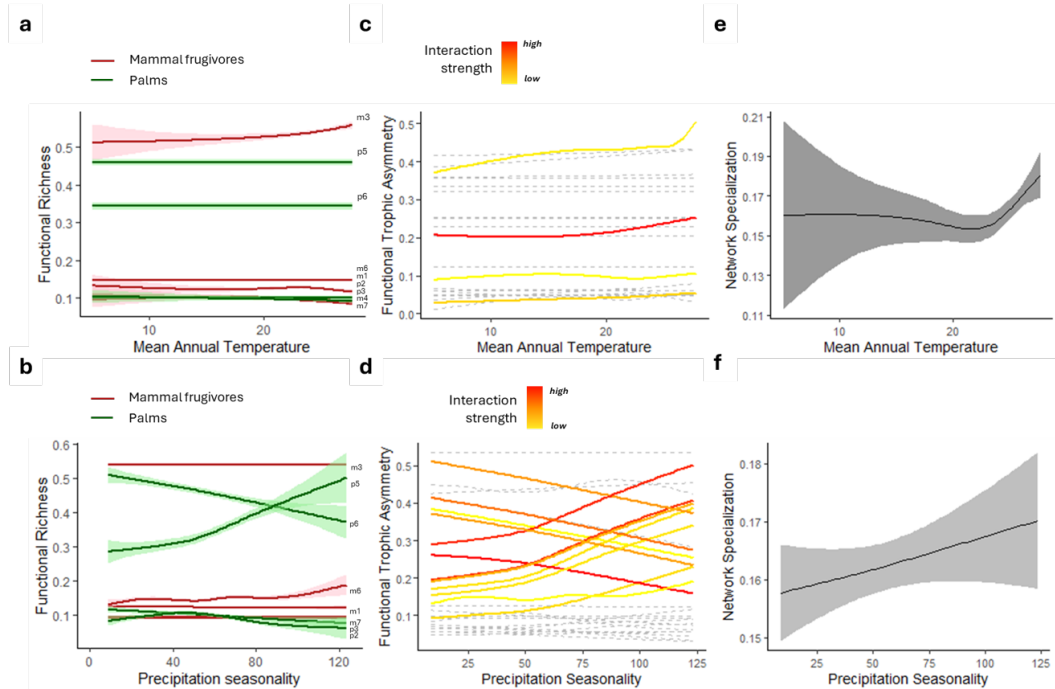


Figure 5: Relationships between environmental gradients, functional diversity, and network properties in the multitrophic system of mutualistic palm-mammal frugivore networks in Neotropics. (a, b) Trends in the functional richness of palms (green) and mammals (red) as a function of mean annual temperature (a) and precipitation seasonality (b), with shaded areas representing confidence intervals. Each trendline estimates the change in Functional Richness of an interaction guild. Each interaction guild corresponds to the species groupings found with the Stochastic Block Model and it is identified with labels at the higher end of the climatic gradient. (c, d) Functional trophic asymmetry (FTA) across temperature (c) and precipitation seasonality (d) for all combinations of potential interactions among and within guilds. Interaction strength indicated by a color gradient from yellow (low) to red (high). Trendlines for interaction guild combinations which are significantly affected with the changes in the climatic gradient are colored and shown in continuous lines. Trendlines for interaction guild combinations which are not responsive to climate are shown in gray and stippled lines. (e, f) Network specialization (z-score) along gradients of mean annual temperature (e) and precipitation seasonality (f), with shaded areas denoting confidence intervals. Network specialization is measured with the specialization index ( $H'$ ), rarefied to be measured in networks of the same number of interactions, and z-score standardized for networks across sites by using a null model that simulates stochastic multispecies assembly.

#### 408 0.3.4 Does interaction strength mediates the influence of climate on 409 FTA?

410 The strength of interaction between guilds of consumers and producers had an over-  
411 all positive effect on FTA (Figure S6). FTA values showed a bi-modal distribution  
412 with peaks at high and low ends of the interaction strength spectrum. However, we

413 did not find strong evidence supporting that the relationship between FTA and cli-  
 414 mate depends on the strength of interaction between interaction guilds ( $F = 746$ ,  $P$   
 415  $> 0.05$ ). The interaction term between guild interaction strength and precipitation  
 416 seasonality had a marginally significant, and positive, effect on FTA. ( $F = 0.14$ ,  $P$   
 417  $= 0.051$ ) (Table 1). Assessing the relationship between FTA' and H2' We found that  
 418 palm-mammalian frugivore networks have moderate levels of trophic specialization  
 419 ( $H2'$ ) ranging from 0.12 to 0.25, where 0 means species have no preference or special-  
 420 lization in their interaction partners and 1 represents networks where each species  
 421 interacts only with a specific subset of interaction partners (Figure S7).

422 Geographic variation in  $H2'$  positively relates to variation in FTA' ( $F = 24.36$ ;  $P$   
 423  $< 0.001$ ) ([Figure 6c, 6d](#)) (Figure S7).  $H2'$  also positively relates to the mean annual  
 424 temperature of the atmosphere ( $F = 2.12$ ,  $P = 0.03$ ), however, effect uncertainty  
 425 is stronger in cold regions than in warm regions ([Figure 5e](#)). Similarly,  $H2'$  is pos-  
 426 itively related to precipitation seasonality PS ( $F = 2.29$ ,  $P = 0.02$ ). ([Figure 5f](#))  
 427 Finally, variation in  $H2'$  does not relate to variation in temperature seasonality or  
 428 total annual precipitation (both  $P > 0.05$ ). The deviance explained by this model  
 429 was 17.6%. (Table 2)

**Table 2**Source: [Article Notebook](#)**Parametric coefficients**

	Estimate	Std. Error	t value	p-value
Intercept	0.16	0	86.33	<b>&lt;2e-16</b>

**Smooth Terms**

	edf	Ref.df	F	p-value
FTA = s(sum_fta)	5.97	7.18	24.37	<b>&lt;2e-16</b>
Mean Annual Temperature = s(Temp)	5.86	7.04	2.13	<b>0.04</b>
Precipitation seasonality = s(PS)	5.42	6.56	2.29	<b>0.03</b>
Temperature seasonality = s(TS)	1.00	1.00	0.74	<b>0.39</b>
Total Annual Precipitation = s(Prec)	5.29	6.39	0.93	<b>0.48</b>

Source: [Article Notebook](#)

430

**0.4 Discussion**

431 Our study reveals that producers and consumers differ in their functional responses  
 432 to climatic gradient thereby giving rise to trophic asymmetry (FTA). The degree of  
 433 FTA in palm-mammal frugivore assemblages varies across the Neotropics, with the  
 434 highest value recorded in regions with a warm climate and a seasonal precipitation  
 435 regime. Furthermore, species assemblages with high FTA also exhibited a high level  
 436 of specialization in their trophic interaction networks. Taken together, our results  
 437 suggest that distinct community assembly processes operate simultaneously across  
 438 trophic levels, reinforcing the idea that network assembly emerges from a dynamic  
 439 interplay of bottom-up and top-down processes (Marjakangas et al., 2022; Moretti &  
 440 Legg, 2009; Schleuning et al., 2023) which are context dependent.

441

442 Palms and mammal frugivore assemblages differ in their response to climatic gradi-  
 443 ents across the Neotropics. There is a positive relationship between the functional

richness of mammal assemblages and temperature, mainly driven by an increase in the richness of small-bodied, opportunistic mammal frugivores with broad diets (Figure 5a, Figure S1). Warm regions have high primary productivity, which translates into an abundance of fruits and other resources that support a great diversity of mammal species and interaction traits (Gorczynski et al., 2021; Losada et al., 2024). Among those, small tropical frugivores tend to have narrower climatic niches as they tend to be restricted to the warmest regions. As opposed to larger bodied mammals, they are less suited to cold climatic conditions because they more easily lose heat (Shipley & McGuire, 2024). In addition, in warm regions, small frugivorous mammals invest less energy in thermoregulation and can allocate more energy to feeding and breeding (Arends & McNab, 2001; Merritt, 2010). Higher reproductive rates and shorter generation times over evolutionary time can create opportunities for adaptation or speciation (Allen et al., 2006). Finally, warm, and stable climates over evolutionary time could have lowered extinction rates, allowing these climatically sensitive small frugivore lineages to persist through time (Sandel et al., 2011).

The functional richness of palms does not relate to variation in temperature, but it is negatively related to precipitation seasonality. Palms, being megathermal plants, evolved in and require warm conditions year-round (Eiserhardt et al., 2011; Reichgelt et al., 2018). However, given the overall warm conditions of Neotropics, geographic variation in mean annual temperature exerts little constraints on palm functional richness. Studies show that variations in mean temperature within the tropical-subtropical range affect palm growth rates rather than community composition (Eiserhardt et al., 2011). Unlike temperature, annual precipitation seasonality strongly relates to palm functional richness. When precipitation becomes seasonal, the overall number of palms species tends to decline, and drought-tolerant palm types are more represented in palm assemblages (Eiserhardt et al., 2011; Sousa et al., 2020) (Figure 5b). As such these habitats favor species with water-saving strategies (e.g. large-nuts) over water-spending ones (e.g. fast growth and large leaves) (Eiserhardt et al., 2011; Emilio et al., 2019). In warm and wet habitats, both strategies coexist since water is abundant (Eiserhardt et al., 2011).

Functional Trophic Asymmetry (FTA) varied geographically, peaking in warm regions with highly seasonal precipitation Figure 6. Overall, average annual temperature has a small but positive effect on FTA. This is mainly due to a proportionally greater representation of guilds with small generalist mammals frugivores in assemblages of warm regions relative to the functional richness of interacting palm assemblages. As such, variation in mean annual temperature and its effects on FTA were associated with shifts in the functional richness of mammals rather than shifts in the functional diversity of palms. These results support the view that the mode of assembly in palm-frugivore networks inhabiting the warmest regions of the neotropics is top-down (i.e. consumer-driven) (Albrecht et al., 2018; Dehling et al., 2016, 2022; Marjakangas et al., 2022; Sonne et al., 2016). In contrast, the significant influence of precipitation seasonality on the functional richness of palm assemblages supports the view that the mode of assembly in palm-frugivore networks inhabiting areas with highly seasonal precipitations is bottom-up (producer-driven).

Interaction strength, representing the intensity of the effect that one species has on another within an ecological network, varies significantly across palms and mammal frugivore guilds. Moreover, variation in the strength of interaction between palm-frugivore guilds mediates the response of FTA to precipitation seasonality. Specifically, strongly interacting guilds show a more significant and positive relationship between FTA and precipitation seasonality. In other words, palm species among guilds with more specialized seed dispersal are more common while palm species among guilds with a generalist seed dispersal strategy become rarer towards regions where rainfall is seasonal (Figure 5b, 5d). As precipitation becomes more seasonal,

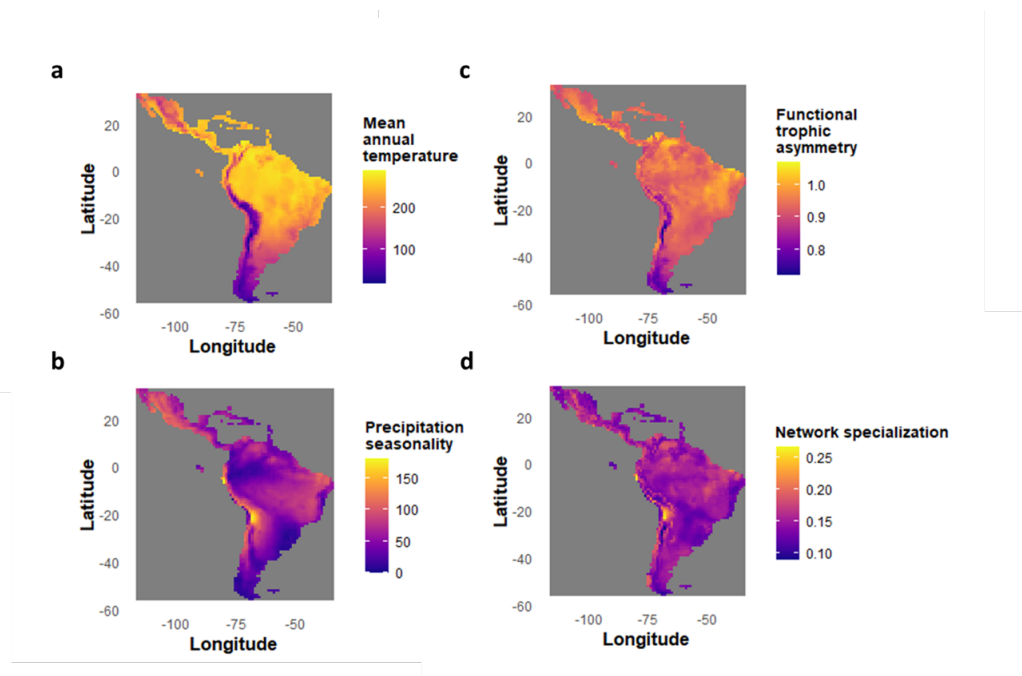


Figure 6: Spatial distribution of climate, functional trophic asymmetry, and network specialization for palm-mammal frugivore seed dispersal networks across the Neotropics. Panels (a) and (b) show the geographical variation in mean annual temperature and precipitation seasonality, respectively, with warmer colors indicating higher values. Panels (c) and (d) depict the spatial patterns of functional trophic asymmetry (FTA) and network specialization ( $H_2'$ ), where higher values are also represented by warmer colors. FTA (Panel c) reflects variation in functional trophic asymmetry across regions, with higher values concentrated in areas of higher temperature and seasonality. Network specialization (Panel d) indicates the degree of exclusive interactions within ecological networks. Color scales for each map are shown in adjacent legends.

498 palm functional richness shifts towards large-fruited species and mammal frugivore  
499 generalists become scarcer. Our results align with findings such as from bat-plant  
500 mutualistic pollination networks, where interacting species exhibit lower niche over-  
501 lap in highly seasonal environments, and for avian-frugivory networks where weaker  
502 trait matching is found towards the tropics (Huang et al., 2025; Schleuning et al.,  
503 2012), but also contrast with others that report stronger trait-matching and interac-  
504 tion strength towards the tropics in plant-hummingbird pollination networks (Sonne  
505 et al., 2020) and avian-palm frugivory (McFadden et al., 2022).

506 The concept of functional trophic asymmetry (FTA) offers a valuable framework to  
507 examine how multitrophic ecological communities respond to shifting environmental  
508 conditions. Our results suggest that as global climate change accelerates, rising tem-  
509 peratures and altered precipitation regimes are likely to increase FTA multitrophic  
510 palm-frugivore communities and increase specialization in palm seed dispersal net-  
511 works. A likely consequence is also the loss of ecosystem function, namely plant func-  
512 tional connectivity —the dispersal of plant propagules between habitat patches—,  
513 which has been shown to decrease with increased specialization and reduced plant  
514 functional diversity (Landim et al., 2025). The same could be true of other ecosys-  
515 tem functions in other types of mutualistic networks, but it remains to be explored  
516 (Acosta-Rojas et al., 2023; Landim et al., 2025; Nowak et al., 2025; Rabeau et al.,  
517 2025). In addition to climate change, habitat fragmentation and human-induced  
518 landscape modifications can independently alter resource and consumer functional  
519 diversity, thereby affecting FTA (Béllo Carvalho et al., 2023; Guevara et al., n.d.).  
520 Although differences in the extent of landscape fragmentation were not directly in-  
521 vestigated in this study, previous research shows that deforestation has a greater  
522 impact on the diversity and redundancy of functional roles in plants than in their  
523 hummingbird pollinators, suggesting a decline in plant functional roles as forests  
524 are lost. Such results reinforce the role of FTA as a key indicator in predicting  
525 shifts in ecosystem function (Bello et al., 2023; Brodie et al., 2021; Montoya & Raf-  
526 faelli, 2010) as species distributions shift in response to climate change (Aizen et  
527 al., 2012; Bartley et al., 2019; Hurtado et al., 2024; Valiente-Banuet et al., 2015).  
528 Adding additional information such as geographical variation in population density,  
529 land-use change, or spatial movement data (e.g., GPS tracking of frugivores) would  
530 improve realism and generalization of our models (Beumer et al., 2025; Borah et al.,  
531 2022; Cousens et al., 2010). Future work can integrate these elements into our data  
532 pipelines once the relevant data becomes available.

533 **0.5 Supplementary material:**  
 534 **0.5.1 Supplementary figures**  
 535 **0.5.2 Figure S1**

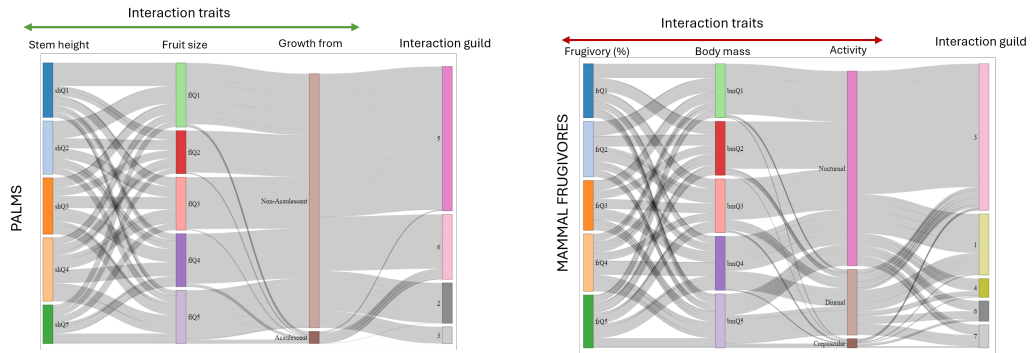


Figure 7: Sankey diagrams illustrating the differences in trait associations to an interaction guild across trophic levels. Top panel - palms: Relationships between stem height and fruit size, followed by a growth form classification (Aculescent vs. Non-Aculescent). Bottom panel-mammal frugivores: Relationships between percentage frugivory in diet and body size categorized into different activity periods (Nocturnal, Diurnal, and Crepuscular). Stem height, Fruit size, Frugivory (%) and Body mass are continuous traits that are grouped into quintiles for visualization purposes. Interaction guilds are defined for both groups with Stochastic Block Modelling of the palm-mammal frugivore interaction aggregated metaweb for the Neotropics. Trait associations to interaction guilds were discovered through multinomial classification modelling using a neural network backend.

### 536 0.5.3 Figure S2

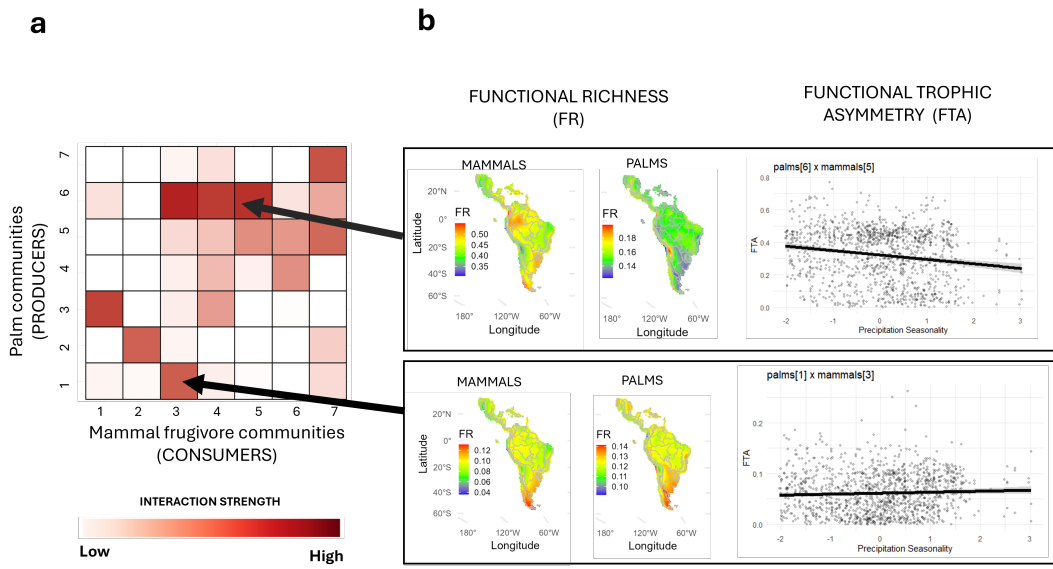


Figure 8: Computing functional asymmetry across distinct interaction guilds. The figure (a) refers to the theta matrix summarizing distinct interaction guilds between producers and consumers with shades of red representing the strength of interactions between species within and between guilds. The figure (b) illustrates two cases of FTA. The panel above illustrates a guild where FTA changes along the environmental gradient (precipitation seasonality, panel below illustrates a case where FTA remains relatively constant )

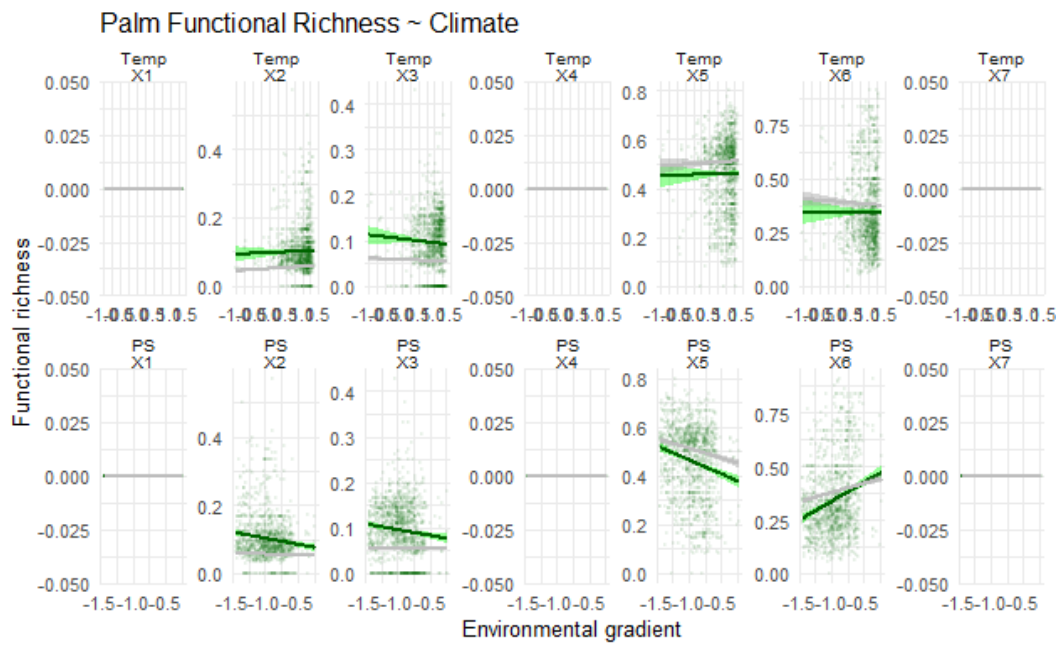
537 **0.5.4 Figure S3**

Figure 9: Changes in the functional richness of palms along gradients of temperature and precipitation seasonality. Each pane represents the trend of the communities of mammals in a single interaction guild. Green lines represent observed trends, gray lines represent expected trends from a null model.

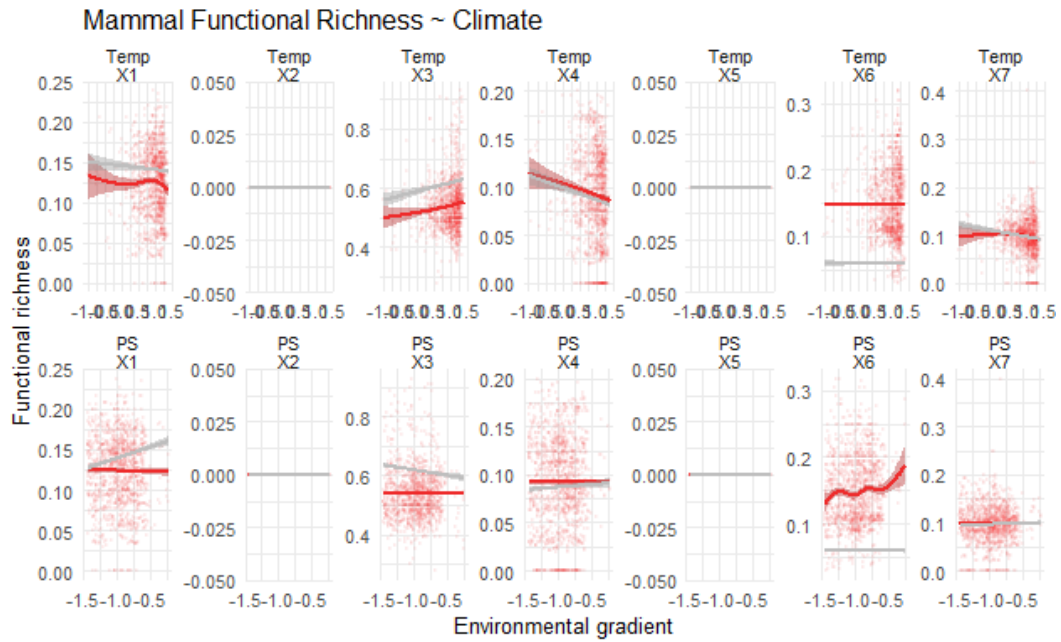
538 **0.5.5 Figure S4**

Figure 10: Changes in the functional richness of mammals along gradients of temperature and precipitation seasonality. Each pane represents the trend of the communities of mammals in a single interaction guild. Red lines represent observed trends, gray lines represent expected trends from a null model

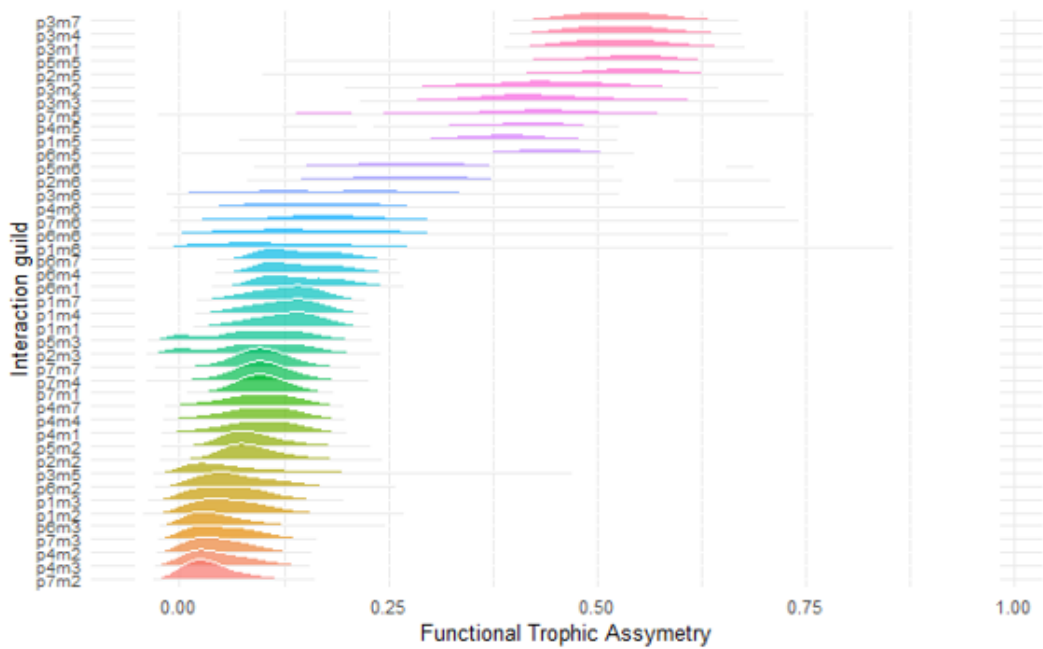
539 **0.5.6 Figure S5**

Figure 11: Functional trophic asymmetry across interaction guilds. Histograms show the distribution of FTA across each combination of palm (p) and mammal (m) guilds across the Neotropics.

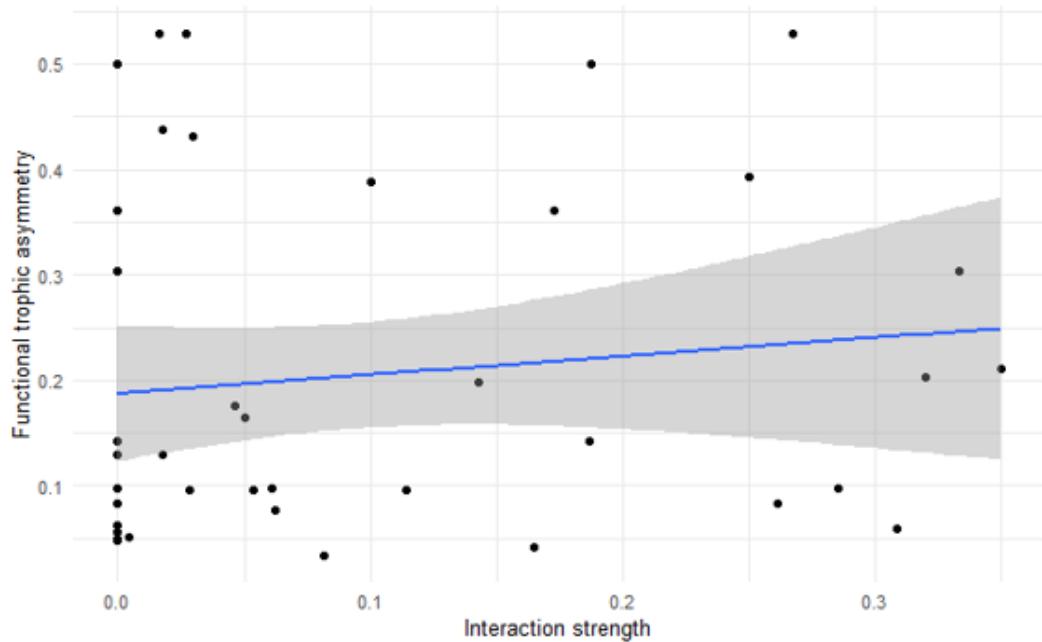
540 **0.5.7 Figure S6**

Figure 12: The relationship between Functional Trophic Asymmetry and Interaction Strength. The y-axis represents the median FTA of an interaction guild. The x-axis represents the interaction strength, measured by their interaction probability between guilds modelled by a stochastic block model (SBM)

541 **0.5.8 Figure S7**

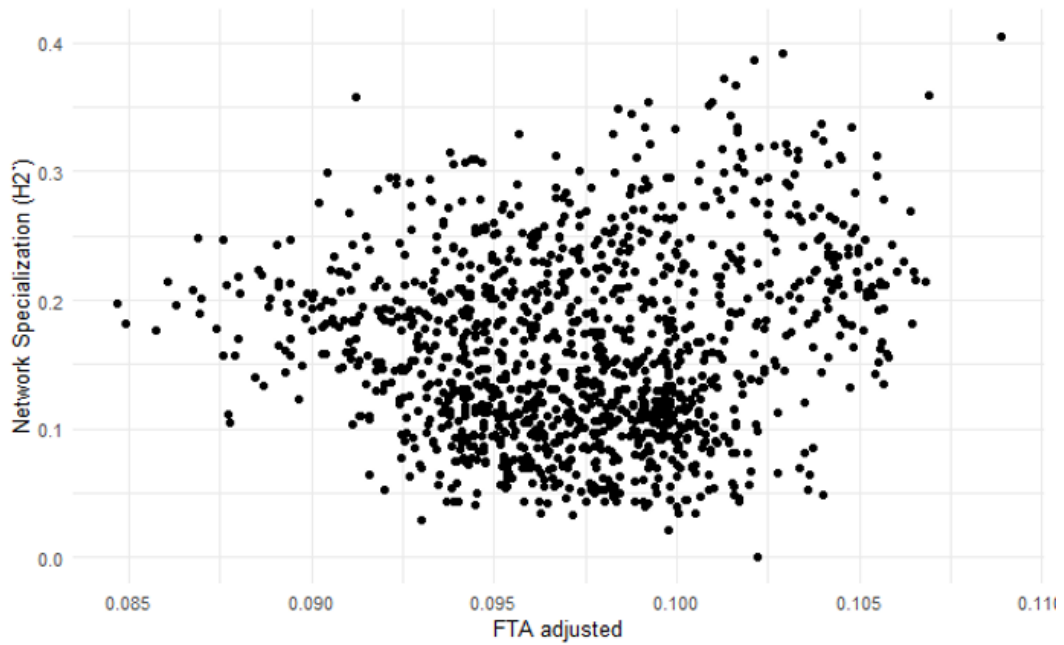


Figure 13: The relationship between Network specialization and FTA (adjusted for interaction strength)

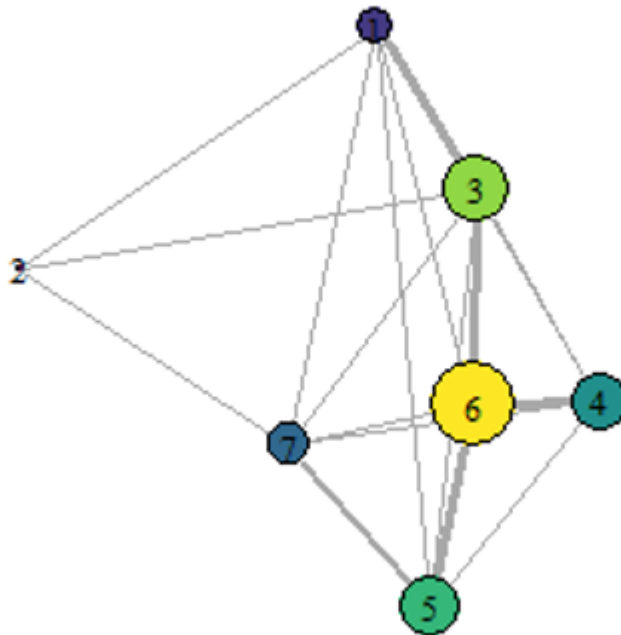
542 **0.5.9 Figure S8**

Figure 14: The relative influence of distinct interaction guilds on maintaining the strupalm-seed dispersal networks in the structure Neotropics. Nodes represent a consumer/producer guild and links represents interactions among them. The size of nodes highlights the node-centrality, a measure of connectivity and influence over other nodes in the network.

543

**0.5.10 Supplementary tables****Table S1**

Summary of parametric and smooth term coefficients for models predicting ecological responses in the Functional Richness of interaction relevant traits of Palms. The parametric coefficients include estimates, standard errors, t-values, and p-values for each predictor (Intercept, Mean annual temperature (Temp), Total annual precipitation (Prec), Temperature seasonality (TS), and Precipitation seasonality (PS)). Smooth terms are shown for each predictor in combination with ecological guilds (Guild\_X1 through Guild\_X7), providing the effective degrees of freedom (edf), reference degrees of freedom (Ref.df), F-statistics, and p-values for each interaction. Significant p-values are highlighted, indicating where predictor-guild interactions have a statistically significant effect on the response variable.

Predictors	Estimates	Dependent variable	
		CI	p
(Intercept)	0.01	-0.01 – 0.03	0.335
Temp	0.00	0.00 – 0.00	<b>0.003</b>
Prec	0.00	-0.00 – 0.00	0.233
TS	-0.00	-0.00 – 0.00	0.789

544

PS	0.00	-0.00 – 0.00	0.499
Smooth term (Temp) × SBM			0.073
GX1			
Smooth term (Temp) × SBM			0.129
GX2			
Smooth term (Temp) × SBM			<b>0.014</b>
GX3			
Smooth term (Temp) × SBM			0.073
GX4			
Smooth term (Temp) × SBM			0.067
GX5			
Smooth term (Temp) × SBM			0.207
GX6			
Smooth term (Temp) × SBM			0.073
GX7			
Smooth term (Prec) × SBM			0.331
GX1			
Smooth term (Prec) × SBM			0.292
GX2			
Smooth term (Prec) × SBM			0.392
GX3			
Smooth term (Prec) × SBM			0.331
GX4			
Smooth term (Prec) × SBM			0.637
GX5			
Smooth term (Prec) × SBM			<b>0.007</b>
GX6			
Smooth term (Prec) × SBM			0.331
GX7			
Smooth term (TS) × SBM			0.864
GX1			
Smooth term (TS) × SBM			0.863
GX2			
Smooth term (TS) × SBM			0.868
GX3			

Smooth term (TS)	0.864
× SBM	
GX4	
Smooth term (TS)	0.890
× SBM	
GX5	
Smooth term (TS)	0.352
× SBM	
GX6	
Smooth term (TS)	0.864
× SBM	
GX7	
Smooth term (PS)	0.705
× SBM	
GX1	
Smooth term (PS)	0.199
× SBM	
GX2	
Smooth term (PS)	0.239
× SBM	
GX3	
Smooth term (PS)	0.705
× SBM	
GX4	
Smooth term (PS)	<b>0.007</b>
× SBM	
GX5	
Smooth term (PS)	<b>0.001</b>
× SBM	
GX6	
Smooth term (PS)	0.705
× SBM	
GX7	
Observations	9009
R <sup>2</sup>	0.012

Source: Article Notebook

546

**Table S2**

Summary of parametric and smooth term coefficients for models predicting ecological responses in the Functional Richness of interaction relevant traits of frugivore Mammals. The parametric coefficients include estimates, standard errors, t-values, and p-values for each predictor (Intercept, Mean annual temperature (Temp), Total annual precipitation (Prec), Temperature seasonality (TS), and Precipitation seasonality (PS) ). Smooth terms are shown for each predictor in combination with ecological guilds (Guild\_X1 through Guild\_X7), providing the effective degrees of freedom (edf), reference degrees of freedom (Ref.df), F-statistics, and p-values for each interaction. Significant p-values are highlighted, indicating where predictor-guild interactions have a statistically significant effect on the response variable.

Predictors (Intercept)	Dependent variable		
	Estimates	CI	p
	0.01	-0.01 – 0.03	0.335

547

Temp	0.00	0.00 – 0.00	<b>0.003</b>
Prec	0.00	-0.00 – 0.00	0.233
TS	-0.00	-0.00 – 0.00	0.789
PS	0.00	-0.00 – 0.00	0.499
Smooth term			0.073
(Temp) × SBM			
GX1			
Smooth term			0.129
(Temp) × SBM			
GX2			
Smooth term			<b>0.014</b>
(Temp) × SBM			
GX3			
Smooth term			0.073
(Temp) × SBM			
GX4			
Smooth term			0.067
(Temp) × SBM			
GX5			
Smooth term			0.207
(Temp) × SBM			
GX6			
Smooth term			0.073
(Temp) × SBM			
GX7			
Smooth term			0.331
(Prec) × SBM			
GX1			
Smooth term			0.292
(Prec) × SBM			
GX2			
Smooth term			0.392
(Prec) × SBM			
GX3			
Smooth term			0.331
(Prec) × SBM			
GX4			
Smooth term			0.637
(Prec) × SBM			
GX5			
Smooth term			<b>0.007</b>
(Prec) × SBM			
GX6			
Smooth term			0.331
(Prec) × SBM			
GX7			
Smooth term (TS)			0.864
× SBM			
GX1			
Smooth term (TS)			0.863
× SBM			
GX2			

Smooth term (TS)	0.868
× SBM	
GX3	
Smooth term (TS)	0.864
× SBM	
GX4	
Smooth term (TS)	0.890
× SBM	
GX5	
Smooth term (TS)	0.352
× SBM	
GX6	
Smooth term (TS)	0.864
× SBM	
GX7	
Smooth term (PS)	0.705
× SBM	
GX1	
Smooth term (PS)	0.199
× SBM	
GX2	
Smooth term (PS)	0.239
× SBM	
GX3	
Smooth term (PS)	0.705
× SBM	
GX4	
Smooth term (PS)	<b>0.007</b>
× SBM	
GX5	
Smooth term (PS)	<b>0.001</b>
× SBM	
GX6	
Smooth term (PS)	0.705
× SBM	
GX7	
Observations	9009
R <sup>2</sup>	0.012

Source: [Article Notebook](#)

549

#### 550 *Supplementary text*

- 551 Acevedo-Quintero, J. F., Zamora-Abrego, J. G., & García, D. (2020). From struc-  
 552 ture to function in mutualistic interaction networks: Topologically important  
 553 frugivores have greater potential as seed dispersers. *Journal of Animal Ecology*,  
 554 89(9), 2181–2191.
- 555 Ackerly, D. D. (2003). Community assembly, niche conservatism, and adaptive evolu-  
 556 tion in changing environments. *International Journal of Plant Sciences*, 164(S3),  
 557 S165–S184.
- 558 Acosta-Rojas, D. C., Barczyk, M. K., Espinosa, C. I., Farwig, N., Homeier, J., Tiede,  
 559 Y., et al. (2023). Abiotic factors similarly shape the distribution of fruit, seed  
 560 and leaf traits in tropical fleshy-fruited tree communities. *Acta Oecologica*, 121,  
 561 103953.

- 562 Aizen, M. A., Sabatino, M., & Tylianakis, J. M. (2012). Specialization and rarity predict nonrandom loss of interactions from mutualist networks. *Science*,  
 563 335(6075), 1486–1489.
- 564 Albrecht, J., Classen, A., Vollstadt, M. G., Mayr, A., Mollel, N. P., Schellenberger  
 565 Costa, D., et al. (2018). Plant and animal functional diversity drive mutualistic  
 566 network assembly across an elevational gradient. *Nature Communications*, 9(1),  
 567 3177.
- 568 Allen, C. R., Garmestani, A., Havlicek, T., Marquet, P. A., Peterson, G., Restrepo,  
 569 C., et al. (2006). Patterns in body mass distributions: Sifting among alternative  
 570 hypotheses. *Ecology Letters*, 9(5), 630–643.
- 571 Allesina, S., Alonso, D., & Pascual, M. (2008). A general model for food web struc-  
 572 ture. *Science*, 320(5876), 658–661.
- 573 Arends, A., & McNab, B. K. (2001). The comparative energetics of ‘caviomorph’ rodents.  
 574 *Comparative Biochemistry and Physiology Part A: Molecular & Integrative Physi-  
 575 ology*, 130(1), 105–122.
- 576 Bartley, T. J., McCann, K. S., Bieg, C., Cazelles, K., Granados, M., Guzzo, M. M.,  
 577 et al. (2019). Food web rewiring in a changing world. *Nature Ecology & Evolu-  
 578 tion*, 3(3), 345–354.
- 579 Bello, C., Schleuning, M., & Graham, C. H. (2023). Analyzing trophic ecosystem  
 580 functions with the interaction functional space. *Trends in Ecology & Evolution*,  
 581 38(5), 424–434.
- 582 B  llo Carvalho, R., Malhi, Y., & Oliveras Menor, I. (2023). Frugivory and seed dis-  
 583 persal in the cerrado: Network structure and defaunation effects. *Biotropica*,  
 584 55(4), 849–865.
- 585 Beumer, L. T., Hertel, A. G., Royaute, R., Tucker, M. A., Albrecht, J., Beltran,  
 586 R., et al. (2025). MoveTraits-a database for integrating animal behaviour into  
 587 trait-based ecology. *bioRxiv*, 2025–03.
- 588 BJORHOLM, S., SVENNING, J.-C., SKOV, F., & BALSLEV, H. (2005). Environmental and  
 589 spatial controls of palm (arecaceae) species richness across the americas. *Global  
 590 Ecology and Biogeography*, 14(5), 423–429.
- 591 Bl  thgen, N., & Klein, A.-M. (2011). Functional complementarity and specialisa-  
 592 tion: The role of biodiversity in plant–pollinator interactions. *Basic and Applied  
 593 Ecology*, 12(4), 282–291.
- 594 Bl  thgen, N., Menzel, F., & Bl  thgen, N. (2006). Measuring specialization in species  
 595 interaction networks. *BMC Ecology*, 6, 1–12.
- 596 Bl  thgen, N., Menzel, F., Hovestadt, T., Fiala, B., & Bl  thgen, N. (2007). Special-  
 597 ization, constraints, and conflicting interests in mutualistic networks. *Current  
 598 Biology*, 17(4), 341–346.
- 599 Bogoni, J. A., Peres, C. A., & Ferraz, K. M. (2020). Extent, intensity and drivers of  
 600 mammal defaunation: A continental-scale analysis across the neotropics. *Sci-  
 601 entific Reports*, 10(1), 14750.
- 602 Borah, D. K., Solanki, G., & Bhattacharjee, P. C. (2022). Seasonal variations in  
 603 home range size of capped langur (*Trachypithecus pileatus*) in a degraded habitat  
 604 in assam, india. *Ecological Questions*, 33(3), 59–66.
- 605 Brodie, J. F., Williams, S., & Garner, B. (2021). The decline of mammal functional  
 606 and evolutionary diversity worldwide. *Proceedings of the National Academy of  
 607 Sciences*, 118(3), e1921849118.
- 608 Cousens, R. D., Hill, J., French, K., & Bishop, I. D. (2010). Towards better predic-  
 609 tion of seed dispersal by animals. *Functional Ecology*, 24(6), 1163–1170.
- 610 Dehling, D. M., Jordano, P., Schaefer, H. M., B  hning-Gaese, K., & Schleuning,  
 611 M. (2016). Morphology predicts species’ functional roles and their degree of spe-  
 612 cialization in plant–frugivore interactions. *Proceedings of the Royal Society B:  
 613 Biological Sciences*, 283(1823), 20152444.
- 614 Dehling, D. M., Bender, I. M., Blendinger, P. G., B  hning-Gaese, K., Mu  oz, M. C.,  
 615 Neuschulz, E. L., et al. (2021). Specialists and generalists fulfil important and

- complementary functional roles in ecological processes. *Functional Ecology*, 35(8), 1810–1821.
- Dehling, D. M., Barreto, E., & Graham, C. H. (2022). The contribution of mutualistic interactions to functional and phylogenetic diversity. *Trends in Ecology & Evolution*, 37(9), 768–776.
- Donoso, I., Schleuning, M., García, D., & Fründ, J. (2017). Defaunation effects on plant recruitment depend on size matching and size trade-offs in seed-dispersal networks. *Proceedings of the Royal Society B: Biological Sciences*, 284(1855), 20162664.
- Donoso, I., Sorensen, M. C., Blendinger, P. G., Kissling, W. D., Neuschulz, E. L., Mueller, T., & Schleuning, M. (2020). Downsizing of animal communities triggers stronger functional than structural decay in seed-dispersal networks. *Nature Communications*, 11(1), 1582.
- Eiserhardt, W. L., Svenning, J.-C., Kissling, W. D., & Balslev, H. (2011). Geographical ecology of the palms (arecaceae): Determinants of diversity and distributions across spatial scales. *Annals of Botany*, 108(8), 1391–1416.
- Emer, C., & Memmott, J. (2023). Intraspecific variation of invaded pollination networks—the role of pollen-transport, pollen-transfer and different levels of biological organization. *Perspectives in Ecology and Conservation*, 21(2), 151–163.
- Emilio, T., Lamarque, L. J., Torres-Ruiz, J. M., King, A., Charrier, G., Burlett, R., et al. (2019). Embolism resistance in petioles and leaflets of palms. *Annals of Botany*, 124(7), 1173–1183.
- Fick, S. E., & Hijmans, R. J. (2017). WorldClim 2: New 1-km spatial resolution climate surfaces for global land areas. *International Journal of Climatology*, 37(12), 4302–4315.
- García, D., Donoso, I., & Rodríguez-Pérez, J. (2018). Frugivore biodiversity and complementarity in interaction networks enhance landscape-scale seed dispersal function. *Functional Ecology*, 32(12), 2742–2752.
- Gevrey, M., Dimopoulos, I., & Lek, S. (2003). Review and comparison of methods to study the contribution of variables in artificial neural network models. *Ecological Modelling*, 160(3), 249–264.
- Gorczynski, D., Hsieh, C., Luciano, J. T., Ahumada, J., Espinosa, S., Johnson, S., et al. (2021). Tropical mammal functional diversity increases with productivity but decreases with anthropogenic disturbance. *Proceedings of the Royal Society B*, 288(1945), 20202098.
- Guevara, E., Duchenne, F., Santander, T., & Graham, C. H. (n.d.). Land use change affects the contribution of niche-based processes to plant-pollinator interactions, with possible consequences for network structure. Available at SSRN 4907880.
- Halpern, B. S., & Floeter, S. R. (2008). Functional diversity responses to changing species richness in reef fish communities. *Marine Ecology Progress Series*, 364, 147–156.
- HilleRisLambers, J., Adler, P. B., Harpole, W. S., Levine, J. M., & Mayfield, M. M. (2012). Rethinking community assembly through the lens of coexistence theory. *Annual Review of Ecology, Evolution, and Systematics*, 43(1), 227–248.
- Hoekstra, F. A., Golovina, E. A., & Buitink, J. (2001). Mechanisms of plant desiccation tolerance. *Trends in Plant Science*, 6(9), 431–438.
- Holt, B. G., Costa, G. C., Penone, C., Lessard, J.-P., Brooks, T. M., Davidson, A. D., et al. (2018). Environmental variation is a major predictor of global trait turnover in mammals. *Journal of Biogeography*, 45(1), 225–237.
- Huang, X., Dalsgaard, B., & Chen, S.-C. (2025). Weaker plant-frugivore trait matching towards the tropics and on islands. *Ecology Letters*, 28(1), e70061.
- Hurtado, P., Aragón, G., Vicente, M., Dalsgaard, B., Krasnov, B. R., & Calatayud, J. (2024). Generalism in species interactions is more the consequence than the cause of ecological success. *Nature Ecology & Evolution*, 8(9), 1602–1611.

- 672 Kissling, W. D., Dormann, C. F., Groeneveld, J., Hickler, T., Kühn, I., McInerny,  
 673 G. J., et al. (2012). Towards novel approaches to modelling biotic interactions  
 674 in multispecies assemblages at large spatial extents. *Journal of Biogeography*,  
 675 39(12), 2163–2178.
- 676 Kissling, W. D., Balslev, H., Baker, W. J., Dransfield, J., Göldel, B., Lim, J. Y.,  
 677 et al. (2019). PalmTraits 1.0, a species-level functional trait database of palms  
 678 worldwide. *Scientific Data*, 6(1), 178.
- 679 Kraft, N. J., & Ackerly, D. D. (2010). Functional trait and phylogenetic tests of  
 680 community assembly across spatial scales in an amazonian forest. *Ecological  
 681 Monographs*, 80(3), 401–422.
- 682 Kraft, N. J., Valencia, R., & Ackerly, D. D. (2008). Functional traits and niche-  
 683 based tree community assembly in an amazonian forest. *Science*, 322(5901),  
 684 580–582.
- 685 Kraft, N. J., Adler, P. B., Godoy, O., James, E. C., Fuller, S., & Levine, J. M.  
 686 (2015). Community assembly, coexistence and the environmental filtering  
 687 metaphor. *Functional Ecology*, 29(5), 592–599.
- 688 Laliberté, E., & Legendre, P. (2010). A distance-based framework for measuring  
 689 functional diversity from multiple traits. *Ecology*, 91(1), 299–305.
- 690 Landim, A. R., Neuschulz, E. L., Donoso, I., Sorensen, M. C., Mueller, T., & Schle-  
 691 uning, M. (2025). Functional connectivity of animal-dispersed plant communities  
 692 depends on the interacting effects of network specialization and resource diver-  
 693 sity. *Proceedings B*, 292(2042), 20242995.
- 694 Lavorel, S. (2013). Plant functional effects on ecosystem services. *Journal of Ecology*.  
 695 Wiley Online Library.
- 696 Losada, M., Suárez-Couselo, M., & Sobral, M. (2024). Geographic distribution of  
 697 mammal diets. *Web Ecology*, 24(2), 71–79.
- 698 Marjakangas, E.-L., Muñoz, G., Turney, S., Albrecht, J., Neuschulz, E. L., Schleun-  
 699 ing, M., & Lessard, J.-P. (2022). Trait-based inference of ecological network  
 700 assembly: A conceptual framework and methodological toolbox. *Ecological  
 701 Monographs*, 92(2), e1502.
- 702 Marques Draxler, C., & Kissling, W. D. (2022). The mutualism–antagonism con-  
 703 tinuum in neotropical palm–frugivore interactions: From interaction outcomes to  
 704 ecosystem dynamics. *Biological Reviews*, 97(2), 527–553.
- 705 McCain, C. M., & King, S. R. (2014). Body size and activity times mediate mam-  
 706 malian responses to climate change. *Global Change Biology*, 20(6), 1760–1769.
- 707 McFadden, I. R., Fritz, S. A., Zimmermann, N. E., Pellissier, L., Kissling, W. D.,  
 708 Tobias, J. A., et al. (2022). Global plant-frugivore trait matching is shaped by  
 709 climate and biogeographic history. *Ecology Letters*, 25(3), 686–696.
- 710 Merritt, J. F. (2010). *The biology of small mammals*. JHU Press.
- 711 Messeder, J. V. S., Silveira, F. A., Cornelissen, T. G., Fuzessy, L. F., & Guerra,  
 712 T. J. (2021). Frugivory and seed dispersal in a hyperdiverse plant clade and its  
 713 role as a keystone resource for the neotropical fauna. *Annals of Botany*, 127(5),  
 714 577–595.
- 715 Montoya, J. M., & Raffaelli, D. (2010). Climate change, biotic interactions and  
 716 ecosystem services. *Philosophical Transactions of the Royal Society B: Biological  
 717 Sciences*, 365(1549), 2013–2018.
- 718 Moretti, M., & Legg, C. (2009). Combining plant and animal traits to assess commu-  
 719 nity functional responses to disturbance. *Ecography*, 32(2), 299–309.
- 720 Muñoz, G., Trøjelsgaard, K., & Kissling, W. D. (2019). A synthesis of animal-  
 721 mediated seed dispersal of palms reveals distinct biogeographical differences  
 722 in species interactions. *Journal of Biogeography*, 46(2), 466–484.
- 723 Nowak, L., Fricke, E. C., Traveset, A., & Donoso, I. (2025). Impacts of species intro-  
 724 ductions on the trait diversity of interacting avian frugivores and fleshy-fruited  
 725 plants depend on native trait diversity. *bioRxiv*, 2025–01.

- 726 Onstein, R. E., Carter, R. J., Xing, Y., & Linder, H. P. (2014). Diversification rate  
 727 shifts in the cape floristic region: The right traits in the right place at the right  
 728 time. *Perspectives in Plant Ecology, Evolution and Systematics*, 16(6), 331–340.
- 729 Onstein, R. E., Baker, W. J., Couvreur, T. L., Faurby, S., Svenning, J.-C., &  
 730 Kissling, W. D. (2017). Frugivory-related traits promote speciation of tropical  
 731 palms. *Nature Ecology & Evolution*, 1(12), 1903–1911.
- 732 Paine, C. T., Baraloto, C., Chave, J., & Hérault, B. (2011). Functional traits of indi-  
 733 vidual trees reveal ecological constraints on community assembly in tropical rain  
 734 forests. *Oikos*, 120(5), 720–727.
- 735 Poisot, T. (2023). Guidelines for the prediction of species interactions through bi-  
 736 nary classification. *Methods in Ecology and Evolution*, 14(5), 1333–1345.
- 737 Rabeau, A., Pigot, A., Tobias, J., & Schleuning, M. (2025). Projected impacts of  
 738 climate change on plant-frugivore interactions across the americas. *bioRxiv*, 2025–  
 739 03.
- 740 Reichgelt, T., West, C. K., & Greenwood, D. R. (2018). The relation between global  
 741 palm distribution and climate. *Scientific Reports*, 8(1), 4721.
- 742 Rohr, R. P., Scherer, H., Kehrli, P., Mazza, C., & Bersier, L.-F. (2010). Modeling  
 743 food webs: Exploring unexplained structure using latent traits. *The American  
 744 Naturalist*, 176(2), 170–177.
- 745 Sandel, B., Arge, L., Dalsgaard, B., Davies, R., Gaston, K., Sutherland, W., & Sven-  
 746 ning, J.-C. (2011). The influence of late quaternary climate-change velocity on  
 747 species endemism. *Science*, 334(6056), 660–664.
- 748 Saravia, L. A., Marina, T. I., Kristensen, N. P., De Troch, M., & Momo, F. R.  
 749 (2022). Ecological network assembly: How the regional metaweb influences lo-  
 750 cal food webs. *Journal of Animal Ecology*, 91(3), 630–642.
- 751 Schleuning, M., Fründ, J., Klein, A.-M., Abrahamszyk, S., Alarcón, R., Albrecht, M.,  
 752 et al. (2012). Specialization of mutualistic interaction networks decreases toward  
 753 tropical latitudes. *Current Biology*, 22(20), 1925–1931.
- 754 Schleuning, M., García, D., & Tobias, J. A. (2023). Animal functional traits: To-  
 755 wards a trait-based ecology for whole ecosystems. *Functional Ecology*. Wiley  
 756 Online Library.
- 757 Seibold, S., Cadotte, M. W., MacIvor, J. S., Thorn, S., & Müller, J. (2018). The  
 758 necessity of multitrophic approaches in community ecology. *Trends in Ecology &  
 759 Evolution*, 33(10), 754–764.
- 760 Shipley, B. R., & McGuire, J. L. (2024). The environmental conditions of endemism  
 761 hotspots shape the functional traits of mammalian assemblages. *Proceedings of  
 762 the Royal Society B*, 291(2018), 20232773.
- 763 Sonne, J., Martín González, A. M., Maruyama, P. K., Sandel, B., Vizentin-Bugoni,  
 764 J., Schleuning, M., et al. (2016). High proportion of smaller ranged hummingbird  
 765 species coincides with ecological specialization across the americas. *Proceedings  
 766 of the Royal Society B: Biological Sciences*, 283(1824), 20152512.
- 767 Sonne, J., Vizentin-Bugoni, J., Maruyama, P. K., Araujo, A. C., Chávez-González,  
 768 E., Coelho, A. G., et al. (2020). Ecological mechanisms explaining interactions  
 769 within plant–hummingbird networks: Morphological matching increases towards  
 770 lower latitudes. *Proceedings of the Royal Society B*, 287(1922), 20192873.
- 771 Sousa, T. R., Schietti, J., Coelho de Souza, F., Esquivel-Muelbert, A., Ribeiro, I.  
 772 O., Emílio, T., et al. (2020). Palms and trees resist extreme drought in amazon  
 773 forests with shallow water tables. *Journal of Ecology*, 108(5), 2070–2082.
- 774 Strydom, A., Mellet, J., Van Rensburg, J., Viljoen, I., Athanasiadis, A., & Pepper,  
 775 M. S. (2022). Open access and its potential impact on public health—a south  
 776 african perspective. *Frontiers in Research Metrics and Analytics*, 7, 975109.
- 777 Terry, J. C. D., & Lewis, O. T. (2020). Finding missing links in interaction networks.  
 778 *Ecology*, 101(7), e03047.

- 779 Valiente-Banuet, A., Aizen, M. A., Alcántara, J. M., Arroyo, J., Cocucci, A., Galetti,  
780 M., et al. (2015). Beyond species loss: The extinction of ecological interactions in  
781 a changing world. *Functional Ecology*, 29(3), 299–307.
- 782 Villéger, S., Mason, N. W., & Mouillot, D. (2008). New multidimensional functional  
783 diversity indices for a multifaceted framework in functional ecology. *Ecology*,  
784 89(8), 2290–2301.
- 785 Wilman, H., Belmaker, J., Simpson, J., Rosa, C. de la, Rivadeneira, M. M., & Jetz,  
786 W. (2014). EltonTraits 1.0: Species-level foraging attributes of the world's birds  
787 and mammals: Ecological archives E095-178. *Ecology*, 95(7), 2027–2027.
- 788 Wood, S. (2017). Mgcv-package mixed GAM computation vehicle with GCV/AIC/REML  
789 smoothness estimation and GAMMs by REML/PQL. *Docs. W3cub. Com.*